iScience

CellPress
OPEN ACCESS

Article

Exocyst complex component 2 is a potential host factor for SARS-CoV-2 infection

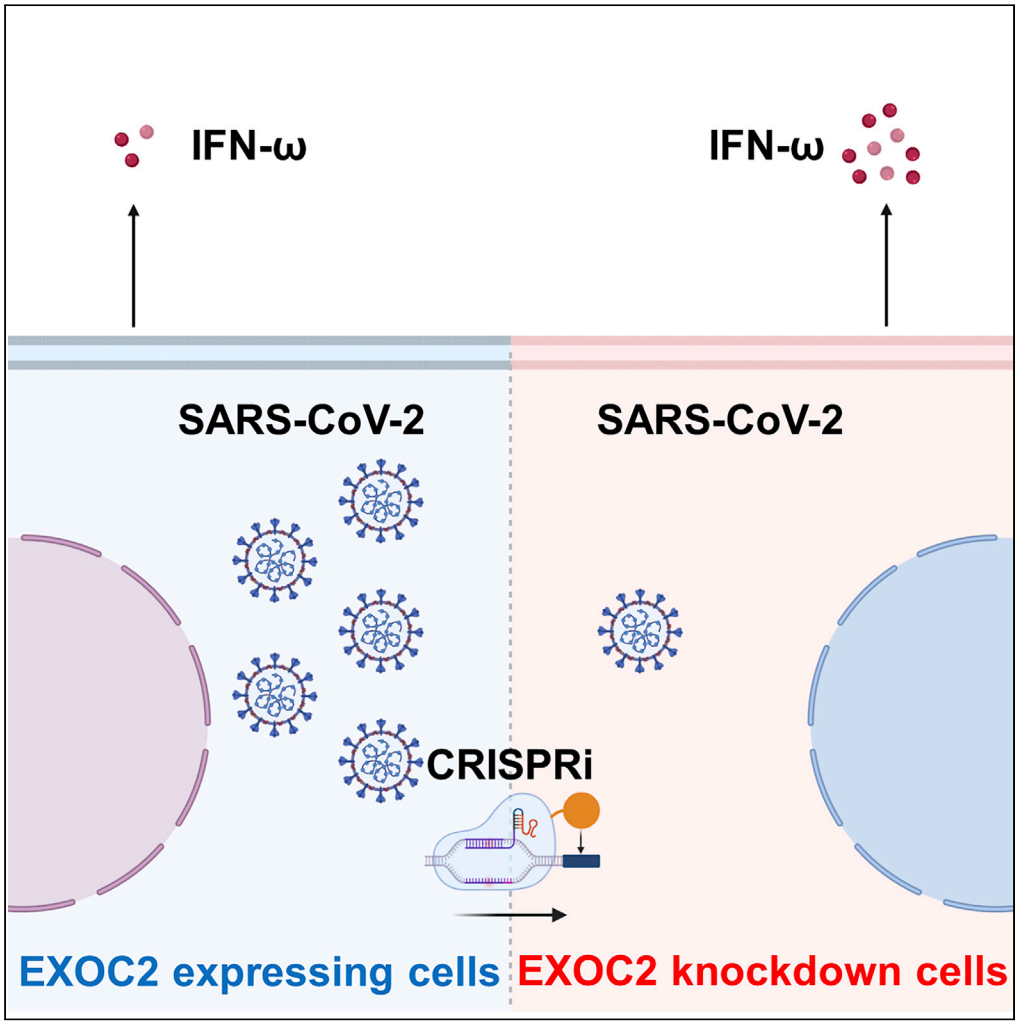

Renxing Yi, Rina Hashimoto, Ayaka Sakamoto, Yasufumi Matsumura, Miki Nagao, Kazutoshi Takahashi, Kazuo Takayama

kazuo.takayama@cira.kyoto-u.ac.jp

Highlights

EXOC2 is one important host factor for SARS-CoV-2 infection

SARS-CoV-2 infection can be inhibited by EXOC2 knockdown

EXOC2 knockdown downregulates SARS-CoV-2 infection by regulating IFNW1 expression

Cytochalasin D significantly decreased the SARS-CoV-2 infection efficiency

Yi et al., iScience 25, 105427
November 18, 2022
https://doi.org/10.1016/j.isci.2022.105427

iScience

CellPress
OPEN ACCESS

Article

Exocyst complex component 2 is a potential host factor for SARS-CoV-2 infection

Renxing Yi,[1] Rina Hashimoto,[1] Ayaka Sakamoto,[1] Yasufumi Matsumura,[2] Miki Nagao,[2] Kazutoshi Takahashi,[1] and Kazuo Takayama[1,3,4,*]

SUMMARY

Severe acute respiratory syndrome coronavirus 2 (SARS-CoV-2) has caused an epidemic and spread rapidly all over the world. Because the analysis of host factors other than receptors and proteases has not been sufficiently performed, we attempted to identify and characterize host factors essential for SARS-CoV-2 infection using iPS cells and airway organoids (AO). Based on previous CRISPR screening and RNA-seq data, we found that exocyst complex component 2 (EXOC2) is one important host factor for SARS-CoV-2 infection. The intracellular SARS-CoV-2 nucleocapsid (N) expression level was decreased to 3.7% and the virus copy number in cell culture medium was decreased to 1.6% by EXOC2 knockdown. Consistently, immunostaining results showed that N protein-positive cells were significantly decreased by EXOC2 knockdown. We also found that EXOC2 knockdown downregulates SARS-CoV-2 infection by regulating IFNW1 expression. In conclusion, controlling the EXOC2 expression level may prevent SARS-CoV-2 infection and deserves further study.

INTRODUCTION

The coronavirus disease 2019 (COVID-19) pandemic has been caused by severe acute respiratory syndrome coronavirus 2 (SARS-CoV-2) and remains a severe threat to public health with millions of deaths. SARS-CoV-2 causes severe life-threatening diseases, including acute respiratory distress syndrome, which can cause dysfunction of the immune system and multi-organ failure.[1] Although several commercial COVID-19 drugs have been successfully developed,[2-4] confirmed cases keep increasing due to viral variants, which highlight the need to elaborate on the mechanisms that underlie SARS-CoV-2 infection to support the development of therapeutics.

SARS-CoV-2 infects human cells through its spike protein, binding to the cell surface protein angiotensin-converting enzyme 2 (ACE2), which induces a conformational change in the S1 subunit and exposes the S2′ site in the S2 subunit.[5] It is known that the S2′ site is cleaved by transmembrane serine protease 2 (TMPRSS2) on the cell surface, which leads to the fusion of the viral membrane and host cell membrane.[6,7] It is also known that, when the S2′ site is not recognized by TMPRSS2, cathepsins in the endosomes will cleave the site and trigger clathrin-mediated endocytosis for viral entry.[5] In addition, furin-like proteases are required for virion maturation in the Golgi by the cleavage of a multibasic site at the S1-S2 junction.[6] Many COVID-19 therapeutic agents have been developed focusing on receptors and proteases related to S protein. However, variants with sequence mutations in their proteins limit the application of those therapeutics. Considering that drugs that can regulate the host response in patients with COVID-19 in a variant-independent manner have not been sufficiently developed, it is important to identify host factors and carry out subsequent drug discovery research.

In the last decade, the CRISPR interference (CRISPRi) system[8] has been proven a powerful tool to not only suppress the expression level of target genes but also for gene screening in specific biological scenarios. In the present study, the CRISPRi system, in which doxycycline (DOX)-inducible catalytically dead Cas9 (dCas9) is fused to a Krüppel-associated box (KRAB) transcriptional repression domain, was applied to screen and validated potential host factors for SARS-CoV-2 infection in human-induced pluripotent stem (iPS) cells.[9,10] Human iPS cells are a useful resource because they are capable of differentiating into somatic cells[11] and are also suitable for efficient genome editing experiments. However, human iPS cells partially lack the innate immune response system, which may limit them as models for the physiology of the

[1]Center for iPS Cell Research and Application (CiRA), Kyoto University, Kyoto 606-8507, Japan

[2]Department of Clinical Laboratory Medicine, Graduate School of Medicine, Kyoto University, Kyoto 606-8507, Japan

[3]AMED-CREST, Japan Agency for Medical Research and Development (AMED), Tokyo 100-0004, Japan

[4]Lead contact

*Correspondence: kazuo.takayama@cira.kyoto-u.ac.jp

https://doi.org/10.1016/j.isci.2022.105427

respiratory tract. In addition, inducible TetO promoter is known to be partially silenced in mature somatic cells differentiated from human iPS cells;[9] thus, it is difficult to use the CRISPRi system in human iPS cell derivatives to evaluate the function of potential host factors for SARS-CoV-2 infection. Since the main cells infected by SARS-CoV-2 are not pluripotent stem cells but respiratory epithelial cells, we also analyzed the function of host factors using airway organoids (AO) in this study.

Using the CRISPRi system, iPS cells, and AO, we searched for essential SARS-CoV-2 host factors and found that exocyst complex component 2 (EXOC2) has an important role in SARS-CoV-2 infection. Then, we elucidated the mechanism of the EXOC2 knockdown-mediated antiviral effect and discovered that this effect is due to an increase of the interferon omega-1 (IFNW1) expression level. Our findings indicate EXOC2 is a potential target for drug development and for understanding the molecular mechanisms of SARS-CoV-2 infection.

RESULTS

SARS-CoV-2 host factor screening

Although many host factors have been identified in previous studies, the validation and detailed functional analysis of these genes have not been sufficiently performed. Therefore, we collected data from 6 published papers[12-17] that all performed CRISPR screening and picked up 51 genes based on the their antiviral effects (Figure S1) to identify host factors required for SARS-CoV-2 infection (Figure 1A). To focus on genes with high endogenous gene expression levels, the top 15 genes were selected based on RNA-seq data that we previously obtained in iPS cells.[18] In the next step, these 15 genes, whose gene expression levels changed significantly by SARS-CoV-2 infection, were examined in iPS cells and AO (Figure S2). We found that the gene expression levels of *EXOC2*, *RAD54L2*, *DRG1*, and *ARID1A* were significantly increased by the SARS-CoV-2 infection. To validate the role of these four genes in the infection, we investigated whether reducing their expression level affects the SARS-CoV-2 infection efficiency in AO by siRNA transfection (Figure 1B). The viral copy number in the culture medium of all groups was decreased by the siRNA transfection (Figure 1C), but EXOC2 knockdown showed the strongest infection inhibitory effect (0.4% that of the control group). Consistently, immunostaining data showed that SARS-CoV-2 nucleocapsids (N)-positive cells were decreased by EXOC2 knockdown (Figure 1D). These results suggested that EXOC2 could be a potential host factor for SARS-CoV-2 infection.

Establishment of EXOC2 knockdown iPS cells

EXOC2 is ubiquitously expressed in many organs and encodes Sec5 protein, which is one of the subunits of the exocyst complex. The exocyst complex is essential for exocytosis by tethering exocytic vesicles from the Golgi to the plasma membrane[19] and promoting the membrane fusion by SNARE complex.[20] The previous genome-wide CRISPR screening study has shown that EXOC2 is one of a potential host factor for the SARS-CoV-2 infection.[13] We therefore decided to further investigate this gene in detail.

Human iPS cells are valuable models for many diseases. Further, since they have pluripotency and differentiation capacity,[11] their genome can be easily edited by using the CRISPR-Cas9 system. Because iPS cells hardly express ACE2, we established ACE2-expressing WTB CRISPRi Gen1 iPS cells equipped with the CRISPRi system.[9] The susceptibility of ACE2-expressing iPS cells to SARS-CoV-2 infection was confirmed by qPCR analysis (Figure S3). Next, we generated tunable and reversible EXOC2-knockdown iPS cells (Figure 2A). Short guide RNA (sgRNA)-expressing colonies were selected based on mKate2 fluorescence signaling (Figure 2B). The EXOC2 sgRNA sequences used in this experiment are summarized in Figure 2C. To confirm the efficiency of the CRISPRi system, the gene expression level of *EXOC2* was examined by qRT-PCR. As expected, the *EXOC2* expression level was sufficiently decreased by DOX treatment (Figure 2D). Additionally, we confirmed that the gene expression levels of other key host factors (*ACE2* and *TMPRSS2*) (Figure 2E) and pluripotent markers (*NANOG*, *OCT3/4*, and *SOX2*) (Figure 2F) were not affected by EXOC2 knockdown. Taken together, we successfully generated EXOC2-knockdown iPS cells that can be infected by SARS-CoV-2.

SARS-CoV-2 infection can be controlled by regulating EXOC2 expression in iPS cells

After successfully generating EXOC2-knockdown iPS cells, we examined whether CRISPRi-based EXOC2 knockdown could affect the SARS-CoV-2 infection in iPS cells (Figure 3A). In agreement with the result of the siRNA-based EXOC2 knockdown (Figure 1C), the SARS-CoV-2 mRNA expression level (Figure 3B)

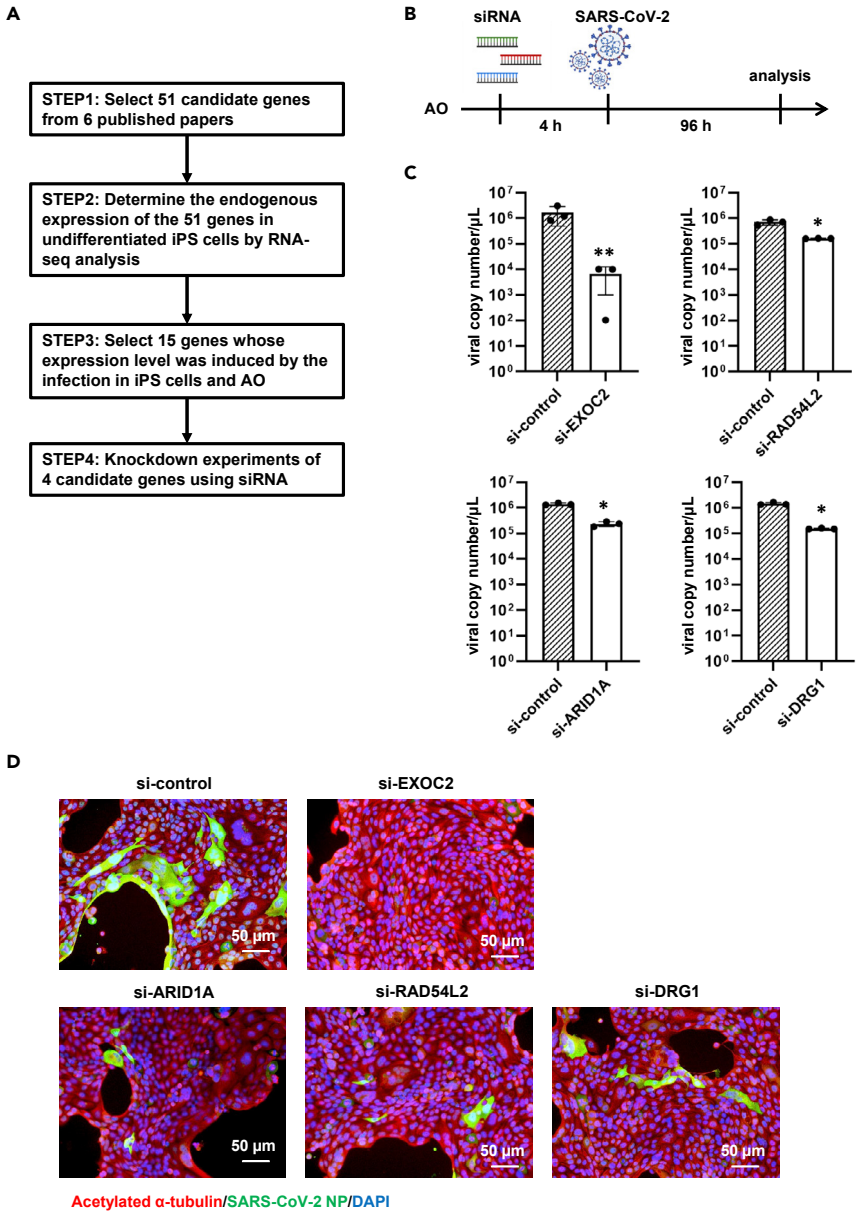

Figure 1. Screening to identify essential host factors for SARS-CoV-2 infection

(A) Schematic diagram of screening.

(B) Airway organoids (AO) were transfected with siRNA (si-control, si-EXOC2, si-RAD54L2, si-ARID1A, or siDRG1) for 4 h and then infected with SARS-CoV-2 (0.1 multiplicity of infection (MOI)).

(C) At 4 dpi, the viral RNA copy number in the cell culture supernatant was measured by qPCR. Unpaired two-tailed Student's *t*-test (*$p < 0.05$, **$p < 0.01$).

(D) Immunofluorescence analysis of SARS-CoV-2 nucleocapsid (N) protein (green) and acetylated α-tubulin (red) in AO. Nuclei were counterstained with DAPI (blue). Data are shown as means ± SD ($n = 3$). See also Figures S1 and S2.

and viral copy number in culture medium (Figure 3C) were significantly decreased to 3.7% and 1.7%, respectively, by EXOC2 knockdown. In addition, SARS-CoV-2 N-positive cells were decreased by EXOC2 knockdown (Figure 3D). Given that cell viability was approximately 70% after EXOC2 knockdown (Figure 3E), we concluded that the antiviral effect was the consequence of EXOC2 knockdown rather than EXOC2 knockdown-mediated cell death. Subsequently, the antiviral effect by EXOC2 knockdown in four SARS-CoV-2 variants: B.1.1.214, BA.1, BA.2, and B.1.617.2 was confirmed, indicating that EXOC2 is necessary for the infection of all the tested variants (Figure 3F). We also confirmed that the expression level and

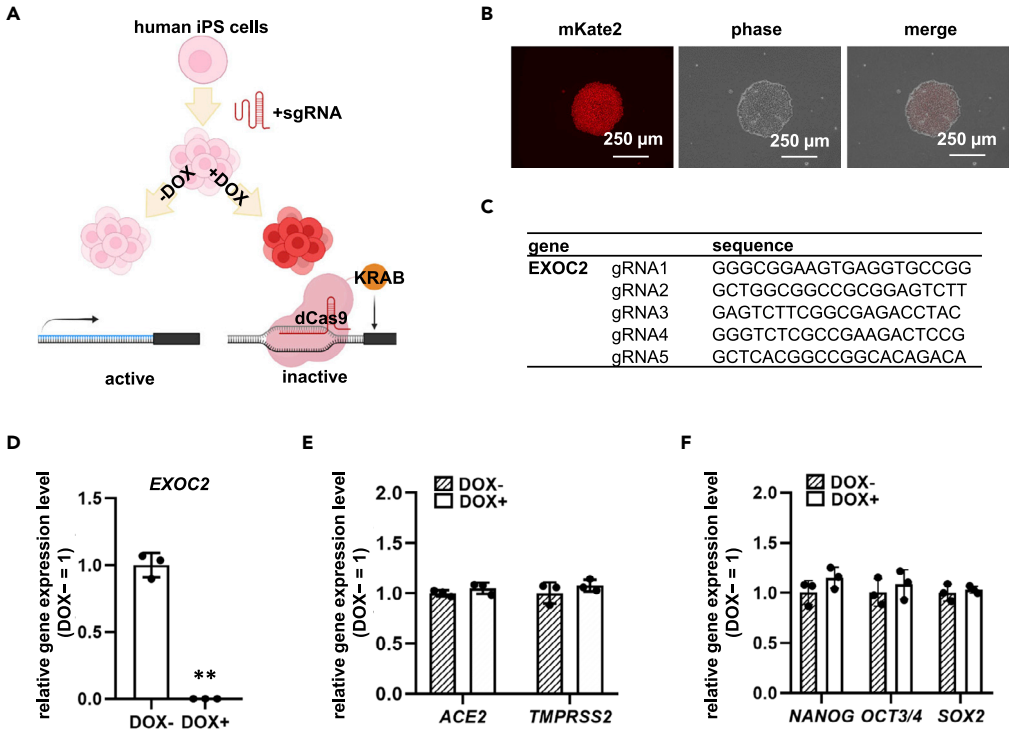

Figure 2. Establishment of EXOC2-knockdown iPS cells

(A) To perform CRISPRi experiments, WTB CRISPRi Gen1 iPS cells that have a DOX-inducible KRAB-dCas9 cassette in the *AAVS1* locus were used. WTB CRISPRi Gen1 iPS cells that constitutively express ACE2 were used to perform the SARS-CoV-2 infection experiments.

(B) EXOC2 sgRNA-expressing WTB CRISPRi Gen1 cells were mKate2-positive. After blasticidin S treatment and single-cell cloning, all iPS cell colonies were mKate2-positive.

(C) EXOC2 sgRNA sequences.

(D) The gene expression levels of *EXOC2* in EXOC2 sgRNA-expressing WTB CRISPRi Gen1 cells treated with or without 1 μM DOX.

(E and F) The gene expression levels of SARS-CoV-2-related genes (*ACE2* and *TMPRSS2*) (E) and pluripotent markers (*NANOG*, *OCT3/4*, and *SOX2*) (F) in sgRNA-EXOC2-expressing WTB CRISPRi Gen1 cells were not changed by the presence of 1 μM DOX. Unpaired two-tailed Student's *t*-test (**$p < 0.01$). Data are shown as means ± SD ($n = 3$). See also Figure S3.

localization of ACE2 were not changed by EXOC2 knockdown (Figure S4), suggesting that the antiviral effect of EXOC2 knockdown is not mediated by the alteration of ACE2 expression level or localization.

To further investigate the function of EXOC2 in SARS-CoV-2 infection, we examined whether exogenous EXOC2 affects the SARS-CoV-2 infection (Figure 3A). By using the *piggyBac* system, EXOC2-overexpressing iPS cells were established (Figure 3G). Although there was a moderate increase in EXOC2 expression, which may be due to the high endogenous gene expression level, the SARS-CoV-2 mRNA expression level (Figure 3H) and the viral copy number in the culture medium (Figure 3I) were increased much more to 538.1% and 548.2%, respectively, by EXOC2 overexpression. Altogether, these results suggested that SARS-CoV-2 infection could be regulated by controlling the EXOC2 expression in human iPS cells.

It is known that Sec3, Sec5, Sec6, and Sec8 assemble into exocyst subcomplex I, while Sec10, Sec15, Exo70, and Exo84 assemble into exocyst subcomplex II.[21] Both EXOC2/Sec5[22] and EXOC8/Exo84[23] are closely related to innate immune signaling kinase, TBK1. Thus, we expected that EXOC8/Exo84 knockdown can show antiviral effects as well as EXOC2. To examine the antiviral effects of EXOC8/Exo84, we established EXOC8-knockdown iPS cells (Figure S5). The gene expression levels of EXOC8 were significantly decreased in EXOC8/Exo84-knockdown iPS cells after the DOX treatment (Figure S5A). However, the viral copy number in the culture medium and *SARS-CoV-2 N* expression level in human iPS cells were hardly changed by EXOC8 knockdown (Figure S5B). These results suggest that EXOC8 does not play an important role in the

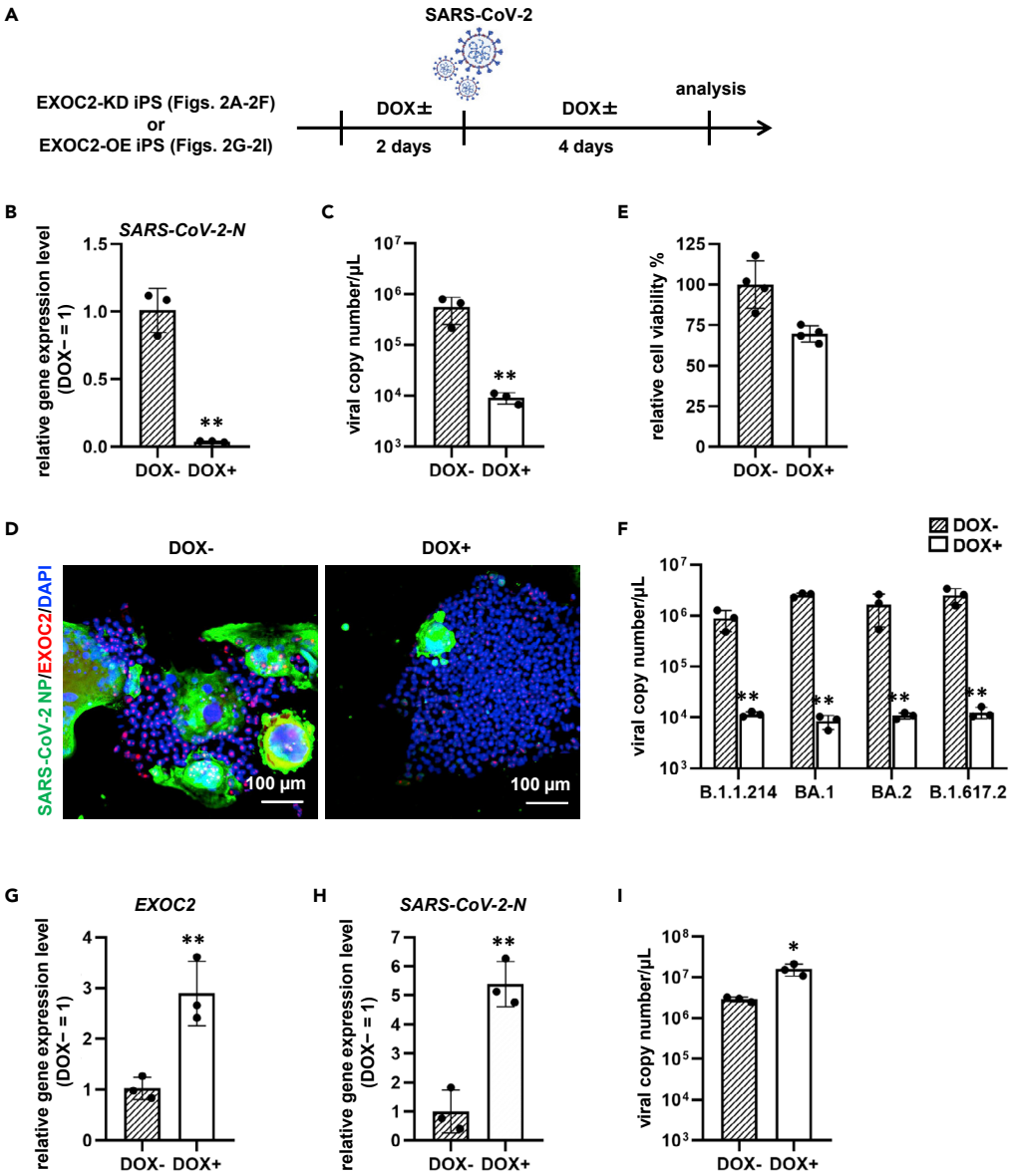

Figure 3. SARS-CoV-2 infection efficiency in iPS cells was increased and decreased by EXOC2 overexpression and knockdown, respectively

(A) EXOC2 sgRNA-expressing WTB-CRISPRi Gen1 cells (EXOC2-KD iPS cells) and TRE3G-EXOC2-expressing WTB-CRISPRi Gen1 cells (EXOC2-OE iPS cells) were cultured with AK02 medium (with or without 1 μM/mL DOX) for 2 days. The cells were then infected with SARS-CoV-2 (0.1 MOI) for 2 h and cultured with AK02 medium (with or without 1 μM/mL DOX) for 4 days. KD, knockdown; OE, overexpression.

(B) The gene expression level of *SARS-CoV-2-N* in EXOC2-KD iPS cells was measured by qRT-PCR.

(C) The viral RNA copy number in the culture supernatant of EXOC2-KD iPS cells was measured by qPCR.

(D) Immunofluorescence analysis of SARS-CoV-2 N protein (green) and EXOC2 (red) in EXOC2-KD iPS cells. Nuclei were counterstained with DAPI (blue).

(E) Cell viability of EXOC2-KD iPS cells was measured by the WST-8 assay.

(F) EXOC2-KD iPS cells were infected with 0.1 MOI SARS-CoV-2 (B.1.1.214, BA.1, BA.2, or B.1.617.2). The viral RNA copy number in the cell culture supernatant was measured by qPCR.

(G) The gene expression level of *EXOC2* in EXOC2-OE iPS cells was measured by qRT-PCR.

(H) The gene expression level of *SARS-CoV-2-N* in EXOC2-OE iPS cells was measured by qRT-PCR.

(I) The viral RNA copy number in the culture supernatant of EXOC2-OE iPS cells was measured by qPCR. Unpaired two-tailed Student's *t*-test (**p < 0.01). Data are shown as means ± SD (*n* = 3 or 4). See also Figures S4 and S5.

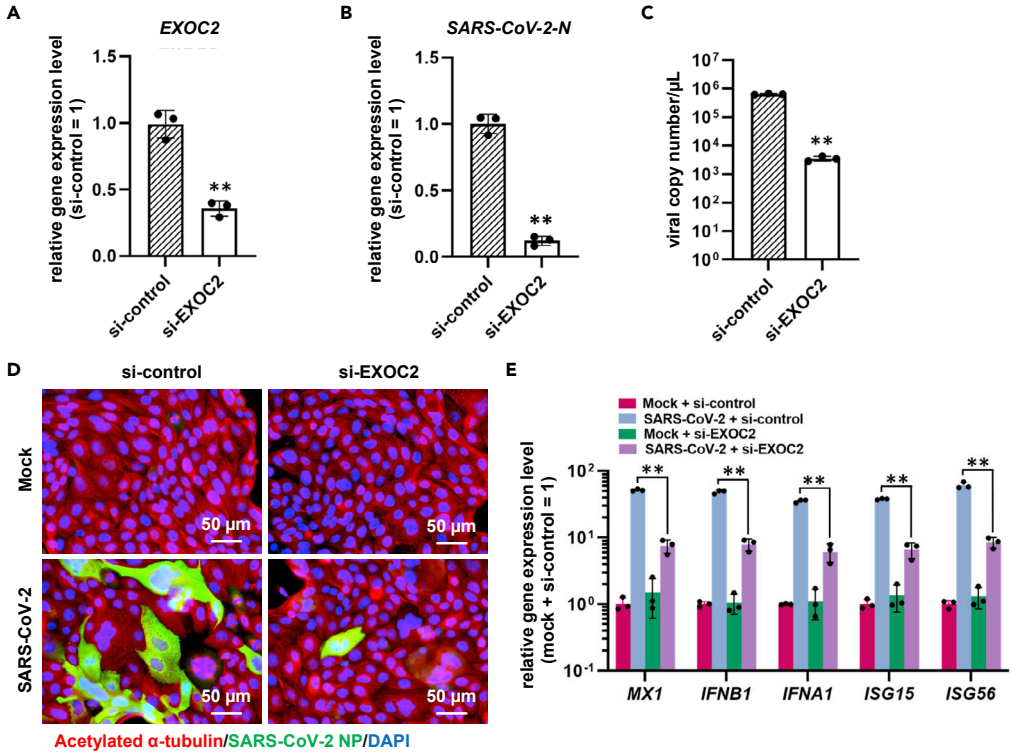

Figure 4. SARS-CoV-2 infection efficiency in AO was decreased by EXOC2 knockdown

AO were dissociated and transfected with siRNA (si-control or si-EXOC2) for 4 h and then infected with SARS-CoV-2 (0.1 MOI).

(A) The gene expression level of *EXOC2* in AO was measured by qRT-PCR. Unpaired two-tailed Student's *t*-test (**$p < 0.01$).

(B) At 4 dpi, the gene expression level of *SARS-CoV-2-N* was measured by qRT-PCR. Unpaired two-tailed Student's *t*-test (**$p < 0.01$).

(C) The viral RNA copy number in the cell culture supernatant was measured by qPCR. Unpaired two-tailed Student's *t*-test (**$p < 0.01$).

(D) Immunofluorescence analysis of SARS-CoV-2 N protein (green) and acetylated α-tubulin (red) in AO. Nuclei were counterstained with DAPI (blue).

(E) The gene expression levels of *MX1*, *IFNB1*, *IFNA1*, *ISG15*, and *ISG56* were measured by qRT-PCR. One-way ANOVA followed by Tukey's post hoc test (**$p < 0.01$). Data are shown as means ± SD ($n = 3$).

SARS-CoV-2 infection. Because there are many exocyst subunits other than EXOC8/Exo84 and EXOC2/Sec5, it will be necessary to clarify their roles in SARS-CoV-2 infection in the future.

EXOC2 is necessary for SARS-CoV-2 infection in airway organoids

Because the respiratory tract is the main organ infected by SARS-CoV-2, we investigated the function of EXOC2 using AO reported in our previous study.[24] EXOC2 expression was downregulated by siRNA transfection (Figure 4A), which again decreased the SARS-CoV-2 mRNA expression level (Figure 4B) and viral copy number in the culture supernatant (Figure 4C). Additionally, SARS-CoV-2 N-positive cells were reduced by EXOC2 knockdown (Figure 4D). AO have innate immune response capacity. We therefore wondered whether the innate immune response caused by the SARS-CoV-2 infection was reduced by EXOC2 knockdown in AO. As expected, the expression levels of *MX1*, *IFNB1*, *IFNA1*, *ISG15*, and *ISG56* were decreased by EXOC2 knockdown, demonstrating that the SARS-CoV-2 infection-mediated innate immune response was reduced by EXOC2 knockdown (Figure 4E). These results indicated that EXOC2 plays an essential role in SARS-CoV-2 infection in AO.

EXOC2 knockdown downregulates SARS-CoV-2 infection by regulating IFNW1 expression

We then elucidated the molecular mechanism of the antiviral effect mediated by EXOC2 expression. Considering that Sec5 is crucial for several innate immune response-related pathways, such as STING

and the TBK1/mTOR cascade,[25,26] we investigated if several genes of the innate immune system are regulated by the EXOC2 expression level. Surprisingly, we found that three types of IFN-related genes, *IFNW1*, *IFNG*, and *IFNL1*, were significantly upregulated by EXOC2 knockdown (Figure 5A), but only IFN-ω exhibited an antiviral effect in TMPRSS2/Vero cells (Figure 5B). Despite IFN-β also showing antiviral activity against SARS-CoV-2, *IFNB1* expression was not affected by EXOC2 knockdown (Figures 5A and 5B). We hypothesized that EXOC2 knockdown upregulated IFNW1 to reduce the SARS-CoV-2 infection efficiency. To verify this hypothesis, we established EXOC2 and IFNW1 double knockdown iPS cells (Figure S6). Remarkably, by checking the viral copy number and SARS-CoV-2 N-positive cells, we found that the antiviral effect by EXOC2 knockdown was negated by the interference of IFNW1 expression (Figures 5C and 5D). In summary, EXOC2 knockdown downregulates SARS-CoV-2 infection efficiency by regulating IFNW1 expression.

F-actin inhibitor reduces SARS-CoV-2 infection efficiency

Based on our findings, we expected drugs that target EXOC2 or its related genes may serve as antiviral drugs against SARS-CoV-2. Because there is no commercially EXOC2 inhibitor available, we decided to utilize drugs that target downstream effectors of EXOC2. SARS-CoV-1 promotes virus replication by actin remolding,[27] and EXOC2/Sec5 interacts with F-actin regulation.[28] Thus, we hypothesized that F-actin inhibitors suppress SARS-CoV-2 infection. Two types of F-actin inhibitors, cytochalasin D, which terminates actin polymerization,[29] and latrunculin B, which prevents F-actin assembly,[30] were used. As expected, treatment with either caused antiviral effects in SARS-CoV-2-infected human iPS cells (Figure S7A) and AO (Figure S7B). However, strong cytotoxicity was observed in the latrunculin B-treated cells, preventing investigation of latrunculin B's antiviral effects. More effective therapeutic agents are expected by further research on genes related to EXOC2.

DISCUSSION

Here, we demonstrated that EXOC2 is necessary for SARS-CoV-2 infection. CRISPRi-based and siRNA-based EXOC2 knockdown decreased the infection efficiency of SARS-CoV-2 in human iPS cells and AO, respectively. EXOC2 knockdown also increased the expression level of IFNW1, which has antiviral effects against SARS-CoV-2 and is one of the reasons for the antiviral effect mediated by EXOC2 knockdown. We also found that the F-actin inhibitor cytochalasin D significantly decreased the SARS-CoV-2 infection efficiency. These findings highlight that EXOC2 is a potential target for clinical therapeutics; especially, pharmacological EXOC2 inhibitors may prevent or reduce the impact of SARS-CoV-2 infection.

EXOC2/Sec5 is one of the subunits of the exocyst complex. It is also known as an effector for small GTPases in the Ras subfamily, RalA and RalB, which are involved in multiple cellular events, such as cell polarization, migration, apoptosis, cytokinesis, autophagy, host defense, tumorigenesis, and metastasis.[26,31,32] However, it is still not clear whether the exocyst complex or other exocyst subunits are necessary for cellular homeostasis. Because cell viability was slightly reduced by EXOC2 knockdown, it is necessary to carefully consider toxicity of this knockdown when conducting drug discovery focusing on EXOC2.

Tunneling nanotubes (TNTs), which are different from other known protrusions (filopodia, microvilli, and dendritic spines), are mainly composed of F-actin and regulated by EXOC2/Sec5.[28] TNTs have been found particularly in immune cells and neuron cell lines[33,34] and were proven to associate with many pathogens, especially viruses, such as HIV, herpesviruses, and influenza A. Importantly, viruses can hijack TNTs to facilitate viral entry, virus trafficking, cell-to-cell spread, and their protection from immune surveillance.[35,36] However, the signaling pathways that control TNT formation seem context dependent, and several EXOC2-independent pathways, such as the Rab35-ACAP2-ARF6-EHD1 cascade in neuron cells[37] and the MAPK pathway in squamous cancer cells,[38] have been reported to control TNT formation. Hence, the potency of drugs targeting TNTs should be investigated in other somatic cells.

Limitations of the study

Our data also showed that EXOC2 knockdown can induce the expression level of IFNW1. However, it is not clear whether EXOC2/Sec5 directly or indirectly acts on IFNW1 expression; thus, further research is required to clarify the relationship between EXOC2 and IFNW1. Finally, because our findings were

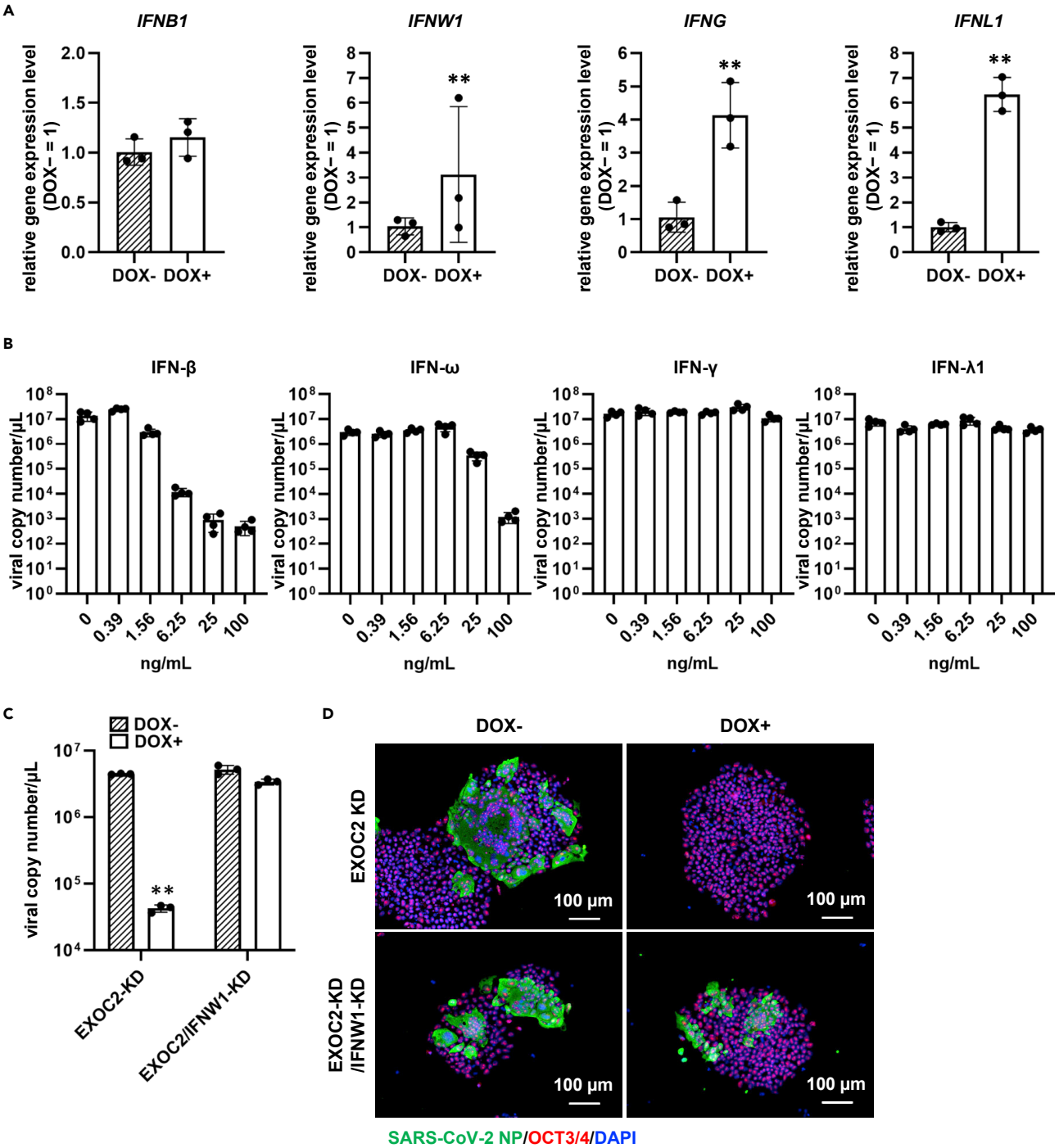

Figure 5. EXOC2 knockdown suppresses SARS-CoV-2 infection efficiency by regulating IFNW1 expression

(A) The gene expression levels of *IFNB1*, *IFNW1*, *IFNG*, and *IFNL1* in EXOC2-KD iPS cells treated with or without 1 μM DOX. Unpaired two-tailed Student's *t*-test (**$p < 0.01$).

(B) TMPRSS2/Vero cells were infected with SARS-CoV-2 (0.1 MOI) for 2 h and cultured with medium containing IFN-β, IFN-ω, IFN-γ, or IFN-λ. At 2 dpi, the viral RNA copy number in the cell culture supernatant was measured by qPCR.

(C) EXOC2-knockdown (KD) iPS cells and EXOC2-KD/IFNW1-KD iPS cells were cultured with AK02N medium containing 1 μM/mL DOX for 2 days and then infected with SARS-CoV-2 (0.1 MOI) for 2 h. At 4 dpi, the viral RNA copy number in the cell culture supernatant was measured by qPCR. One-way ANOVA followed by Tukey's post hoc test (**$p < 0.01$).

(D) Immunofluorescence analysis of SARS-CoV-2 N protein (green) and OCT3/4 (red) in EXOC2-KD or EXOC2-KD/IFNW1-KD iPS cells. Nuclei were counterstained with DAPI (blue). Data are shown as means ± SD ($n = 3$ or 4). See also Figures S6 and S7.

obtained using only *in vitro* models, *in vivo* experiments should also be conducted. Nevertheless, our findings provide a basis for the study of EXOC2 and its related genes to lead to the development of potent COVID-19 therapeutic agents.

STAR★METHODS

Detailed methods are provided in the online version of this paper and include the following:

- KEY RESOURCES TABLE
- RESOURCE AVAILABILITY
  - Lead contact
  - Materials availability
  - Data and code availability
- EXPERIMENTAL MODEL AND SUBJECT DETAILS
  - Ethics statement
  - Cell culture
- METHOD DETAILS
  - Human iPS cells
  - Airway organoids
  - SARS-CoV-2 preparation
  - Viral titration of SARS-CoV-2
  - Drug or IFN treatment
  - Cell viability test
  - Quantification of viral RNA copy number
  - Quantitative PCR
  - siRNA transfection
  - Immunofluorescence staining
  - ACE2-expressing iPS cells
  - Generation of EXOC2-expressing iPS cells
  - CRISPRi experiments in human iPS cells
- QUANTIFICATION AND STATISTICAL ANALYSIS

SUPPLEMENTAL INFORMATION

Supplemental information can be found online at https://doi.org/10.1016/j.isci.2022.105427.

ACKNOWLEDGMENTS

We thank Dr. Peter Karagiannis (Sofia Scientific Writing) for critical reading of the manuscript, Dr. Yoshio Koyanagi, Dr. Takeshi Noda, Dr. Yukiko Muramoto, and Ms. Naoko Misawa (Kyoto University) for the setup and operation of the BSL-3 laboratory at Kyoto University, Dr. Shinya Yamanaka (Kyoto University) for helpful discussions, and Ms. Natsumi Mimura, Ms. Emi Sano, and Ms. Naoko Yasuhara (Kyoto University) for technical assistance. This research was supported by the iPS Cell Research Fund, the COVID-19 Private Fund (to the Shinya Yamanaka Laboratory, CiRA, Kyoto University), the Joint Usage/Research Center Program of Institute for Frontier Life and Medical Sciences Kyoto University, Japan Science and Technology Agency (JST) SPRING (Grant Number JPMJSP2110), and the Japan Agency for Medical Research and Development (AMED) (JP20fk0108533, JP21fk0108492, JP21gm1610005).

AUTHOR CONTRIBUTIONS

R.X. performed the CRISPRi experiments, siRNA experiments, qPCR analyses, data analyses, statistical analysis, and preparation of the manuscript. R.H. performed the SARS-CoV-2 infection experiments, data analyses, and preparation of the manuscript. A.S. performed the iPS cell culture, AO culture, and qPCR analyses. Y.M. collected the clinical samples. M.N. collected the clinical samples. K. Takahashi performed the CRISPRi experiments and data analyses. K. Takayama performed the research design, data analyses, review and editing of the manuscript, funding acquirement, and final approval.

DECLARATION OF INTERESTS

K. Takahashi is on the scientific advisory board of I Peace, Inc. without salary.

Received: July 8, 2022
Revised: September 29, 2022
Accepted: October 19, 2022
Published: November 18, 2022

REFERENCES

1. Mangalmurti, N., and Hunter, C.A. (2020). Cytokine storms: understanding COVID-19. Immunity *53*, 19–25.

2. Beigel, J.H., Tomashek, K.M., Dodd, L.E., Mehta, A.K., Zingman, B.S., Kalil, A.C., Hohmann, E., Chu, H.Y., Luetkemeyer, A., Kline, S., et al. (2020). Remdesivir for the treatment of covid-19. N. Engl. J. Med. *383*, 1813–1826.

3. Cox, R.M., Wolf, J.D., and Plemper, R.K. (2021). Therapeutically administered ribonucleoside analogue MK-4482/EIDD-2801 blocks SARS-CoV-2 transmission in ferrets. Nat. Microbiol. *6*, 11–18.

4. Hammond, J., Leister-Tebbe, H., Gardner, A., Abreu, P., Bao, W., Wisemandle, W., Baniecki, M., Hendrick, V.M., Damle, B., Simón-Campos, A., et al. (2022). Oral nirmatrelvir for high-risk, nonhospitalized adults with covid-19. N. Engl. J. Med. *386*, 1397–1408. https://doi.org/10.1056/NEJMoa2118542.

5. Jackson, C.B., Farzan, M., Chen, B., and Choe, H. (2022). Mechanisms of SARS-CoV-2 entry into cells. Nat. Rev. Mol. Cell Biol. *23*, 3–20.

6. Hoffmann, M., Kleine-Weber, H., and Pöhlmann, S. (2020). A multibasic cleavage site in the spike protein of SARS-CoV-2 is essential for infection of human lung cells. Mol. Cell *78*, 779–784.e5.

7. Hoffmann, M., Kleine-Weber, H., Schroeder, S., Krüger, N., Herrler, T., Erichsen, S., Schiergens, T.S., Herrler, G., Wu, N.-H., Nitsche, A., et al. (2020). SARS-CoV-2 cell entry depends on ACE2 and TMPRSS2 and is blocked by a clinically proven protease inhibitor. Cell *181*, 271–280.e8.

8. Larson, M.H., Gilbert, L.A., Wang, X., Lim, W.A., Weissman, J.S., and Qi, L.S. (2013). CRISPR interference (CRISPRi) for sequence-specific control of gene expression. Nat. Protoc. *8*, 2180–2196.

9. Mandegar, M.A., Huebsch, N., Frolov, E.B., Shin, E., Truong, A., Olvera, M.P., Chan, A.H., Miyaoka, Y., Holmes, K., Spencer, C.I., et al. (2016). CRISPR interference efficiently induces specific and reversible gene silencing in human iPSCs. Cell Stem Cell *18*, 541–553.

10. Hashimoto, R., Sakamoto, A., Deguchi, S., Yi, R., Sano, E., Hotta, A., Takahashi, K., Yamanaka, S., and Takayama, K. (2021). Dual inhibition of TMPRSS2 and Cathepsin Bprevents SARS-CoV-2 infection in iPS cells. Mol. Ther. Nucleic Acids *26*, 1107–1114. https://doi.org/10.1016/j.omtn.2021.10.016.

11. Takahashi, K., Tanabe, K., Ohnuki, M., Narita, M., Ichisaka, T., Tomoda, K., and Yamanaka, S. (2007). Induction of pluripotent stem cells from adult human fibroblasts by defined factors. Cell *131*, 861–872.

12. Wei, J., Alfajaro, M.M., DeWeirdt, P.C., Hanna, R.E., Lu-Culligan, W.J., Cai, W.L., Strine, M.S., Zhang, S.M., Graziano, V.R., Schmitz, C.O., et al. (2021). Genome-wide CRISPR screens reveal host factors critical for SARS-CoV-2 infection. Cell *184*, 76–91.e13. https://doi.org/10.1016/j.cell.2020.10.028.

13. Wang, R., Simoneau, C.R., Kulsuptrakul, J., Bouhaddou, M., Travisano, K.A., Hayashi, J.M., Carlson-Stevermer, J., Zengel, J.R., Richards, C.M., Fozouni, P., et al. (2021). Genetic screens identify host factors for SARS-CoV-2 and common cold coronaviruses. Cell *184*, 106–119.e14. https://doi.org/10.1016/j.cell.2020.12.004.

14. Schneider, W.M., Luna, J.M., Hoffmann, H.H., Sánchez-Rivera, F.J., Leal, A.A., Ashbrook, A.W., Le Pen, J., Ricardo-Lax, I., Michailidis, E., Peace, A., et al. (2021). Genome-scale identification of SARS-CoV-2 and pan-coronavirus host factor networks. Cell *184*, 120–132.e14. https://doi.org/10.1016/j.cell.2020.12.006.

15. Baggen, J., Persoons, L., Vanstreels, E., Jansen, S., Van Looveren, D., Boeckx, B., Geudens, V., De Man, J., Jochmans, D., Wauters, J., et al. (2021). Genome-wide CRISPR screening identifies TMEM106B as a proviral host factor for SARS-CoV-2. Nat. Genet. *53*, 435–444. https://doi.org/10.1038/s41588-021-00805-2.

16. Zhu, Y., Feng, F., Hu, G., Wang, Y., Yu, Y., Zhu, Y., Xu, W., Cai, X., Sun, Z., Han, W., et al. (2021). A genome-wide CRISPR screen identifies host factors that regulate SARS-CoV-2 entry. Nat. Commun. *12*, 961. https://doi.org/10.1038/s41467-021-21213-4.

17. Flynn, R.A., Belk, J.A., Qi, Y., Yasumoto, Y., Wei, J., Alfajaro, M.M., Shi, Q., Mumbach, M.R., Limaye, A., DeWeirdt, P.C., et al. (2021). Discovery and functional interrogation of SARS-CoV-2 RNA-host protein interactions. Cell *184*, 2394–2411.e16. https://doi.org/10.1016/j.cell.2021.03.012.

18. Sano, E., Deguchi, S., Sakamoto, A., Mimura, N., Hirabayashi, A., Muramoto, Y., Noda, T., Yamamoto, T., and Takayama, K. (2021). Modeling SARS-CoV-2 infection and its individual differences with ACE2-expressing human iPS cells. iScience *24*, 102428. https://doi.org/10.1016/j.isci.2021.102428.

19. He, B., and Guo, W. (2009). The exocyst complex in polarized exocytosis. Curr. Opin. Cell Biol. *21*, 537–542. https://doi.org/10.1016/j.ceb.2009.04.007.

20. Heider, M.R., and Munson, M. (2012). Exorcising the exocyst complex. Traffic *13*, 898–907. https://doi.org/10.1111/j.1600-0854.2012.01353.x.

21. Mei, K., and Guo, W. (2018). The exocyst complex. Curr. Biol. *28*. R922–r925. https://doi.org/10.1016/j.cub.2018.06.042.

22. Chien, Y., Kim, S., Bumeister, R., Loo, Y.M., Kwon, S.W., Johnson, C.L., Balakireva, M.G., Romeo, Y., Kopelovich, L., Gale, M., Jr., et al. (2006). RalB GTPase-mediated activation of the IkappaB family kinase TBK1 couples innate immune signaling to tumor cell survival. Cell *127*, 157–170. https://doi.org/10.1016/j.cell.2006.08.034.

23. Uhm, M., Bazuine, M., Zhao, P., Chiang, S.H., Xiong, T., Karunanithi, S., Chang, L., and Saltiel, A.R. (2017). Phosphorylation of the exocyst protein Exo84 by TBK1 promotes insulin-stimulated GLUT4 trafficking. Sci. Signal. *10*, eaah5085. https://doi.org/10.1126/scisignal.aah5085.

24. Sano, E., Suzuki, T., Hashimoto, R., Itoh, Y., Sakamoto, A., Sakai, Y., Saito, A., Okuzaki, D., Motooka, D., Muramoto, Y., et al. (2022). Cell response analysis in SARS-CoV-2 infected bronchial organoids. Commun. Biol. *5*, 516. https://doi.org/10.1038/s42003-022-03499-2.

25. Ishikawa, H., Ma, Z., and Barber, G.N. (2009). STING regulates intracellular DNA-mediated, type I interferon-dependent innate immunity. Nature *461*, 788–792. https://doi.org/10.1038/nature08476.

26. Zaman, A., Wu, X., Lemoff, A., Yadavalli, S., Lee, J., Wang, C., Cooper, J., McMillan, E.A., Yeaman, C., Mirzaei, H., et al. (2021). Exocyst protein subnetworks integrate Hippo and mTOR signaling to promote virus detection and cancer. Cell Rep. *36*, 109491. https://doi.org/10.1016/j.celrep.2021.109491.

27. Wen, Z., Zhang, Y., Lin, Z., Shi, K., and Jiu, Y. (2020). Cytoskeleton-a crucial key in host cell for coronavirus infection. J. Mol. Cell Biol. *12*, 968–979. https://doi.org/10.1093/jmcb/mjaa042.

28. Hase, K., Kimura, S., Takatsu, H., Ohmae, M., Kawano, S., Kitamura, H., Ito, M., Watarai, H., Hazelett, C.C., Yeaman, C., and Ohno, H. (2009). M-Sec promotes membrane nanotube formation by interacting with Ral and the exocyst complex. Nat. Cell Biol. *11*, 1427–1432. https://doi.org/10.1038/ncb1990.

29. Hanna, S.J., McCoy-Simandle, K., Miskolci, V., Guo, P., Cammer, M., Hodgson, L., and Cox, D. (2017). The role of rho-GTPases and actin polymerization during macrophage tunneling nanotube biogenesis. Sci. Rep. *7*, 8547. https://doi.org/10.1038/s41598-017-08950-7.

30. Rostami, J., Holmqvist, S., Lindström, V., Sigvardson, J., Westermark, G.T., Ingelsson,

M., Bergström, J., Roybon, L., and Erlandsson, A. (2017). Human astrocytes transfer aggregated alpha-synuclein via tunneling nanotubes. J. Neurosci. *37*, 11835–11853. https://doi.org/10.1523/jneurosci.0983-17.2017.

31. Simicek, M., Lievens, S., Laga, M., Guzenko, D., Aushev, V.N., Kalev, P., Baietti, M.F., Strelkov, S.V., Gevaert, K., Tavernier, J., and Sablina, A.A. (2013). The deubiquitylase USP33 discriminates between RALB functions in autophagy and innate immune response. Nat. Cell Biol. *15*, 1220–1230. https://doi.org/10.1038/ncb2847.

32. Cascone, I., Selimoglu, R., Ozdemir, C., Del Nery, E., Yeaman, C., White, M., and Camonis, J. (2008). Distinct roles of RalA and RalB in the progression of cytokinesis are supported by distinct RalGEFs. Embo J. *27*, 2375–2387. https://doi.org/10.1038/emboj.2008.166.

33. Marzo, L., Gousset, K., and Zurzolo, C. (2012). Multifaceted roles of tunneling nanotubes in intercellular communication. Front. Physiol. *3*, 72. https://doi.org/10.3389/fphys.2012.00072.

34. Gerdes, H.H., Rustom, A., and Wang, X. (2013). Tunneling nanotubes, an emerging intercellular communication route in development. Mech. Dev. *130*, 381–387. https://doi.org/10.1016/j.mod.2012.11.006.

35. Tiwari, V., Koganti, R., Russell, G., Sharma, A., and Shukla, D. (2021). Role of tunneling nanotubes in viral infection, neurodegenerative disease, and cancer. Front. Immunol. *12*, 680891. https://doi.org/10.3389/fimmu.2021.680891.

36. Jansens, R.J.J., Tishchenko, A., and Favoreel, H.W. (2020). Bridging the gap: virus long-distance spread via tunneling nanotubes. J. Virol. *94*, 021200–e2219. https://doi.org/10.1128/jvi.02120-19.

37. Bhat, S., Ljubojevic, N., Zhu, S., Fukuda, M., Echard, A., and Zurzolo, C. (2020). Rab35 and its effectors promote formation of tunneling nanotubes in neuronal cells. Sci. Rep. *10*, 16803. https://doi.org/10.1038/s41598-020-74013-z.

38. Sáenz-de-Santa-María, I., Bernardo-Castiñeira, C., Enciso, E., García-Moreno, I., Chiara, J.L., Suarez, C., and Chiara, M.D. (2017). Control of long-distance cell-to-cell communication and autophagosome transfer in squamous cell carcinoma via tunneling nanotubes. Oncotarget *8*, 20939–20960. https://doi.org/10.18632/oncotarget.15467.

39. Matsuyama, S., Nao, N., Shirato, K., Kawase, M., Saito, S., Takayama, I., Nagata, N., Sekizuka, T., Katoh, H., Kato, F., et al. (2020). Enhanced isolation of SARS-CoV-2 by TMPRSS2-expressing cells. Proc. Natl. Acad. Sci. USA *117*, 7001–7003. https://doi.org/10.1073/pnas.2002589117.

40. Ishida, K., Xu, H., Sasakawa, N., Lung, M.S.Y., Kudryashev, J.A., Gee, P., and Hotta, A. (2018). Site-specific randomization of the endogenous genome by a regulatable CRISPR-Cas9 piggyBac system in human cells. Sci. Rep. *8*, 310. https://doi.org/10.1038/s41598-017-18568-4.

41. Horlbeck, M.A., Gilbert, L.A., Villalta, J.E., Adamson, B., Pak, R.A., Chen, Y., Fields, A.P., Park, C.Y., Corn, J.E., Kampmann, M., and Weissman, J.S. (2016). Compact and highly active next-generation libraries for CRISPR-mediated gene repression and activation. Elife *5*, e19760. https://doi.org/10.7554/eLife.19760.

42. Takahashi, K., Jeong, D., Wang, S., Narita, M., Jin, X., Iwasaki, M., Perli, S.D., Conklin, B.R., and Yamanaka, S. (2020). Critical roles of translation initiation and RNA uridylation in endogenous retroviral expression and neural differentiation in pluripotent stem cells. Cell Rep. *31*, 107715. https://doi.org/10.1016/j.celrep.2020.107715.

STAR★METHODS

KEY RESOURCES TABLE

REAGENT or RESOURCE	SOURCE	IDENTIFIER
Antibodies		
Donkey anti-Mouse IgG (H+L) highly cross-adsorbed secondary antibody, Alexa fluor plus 594	Thermo Fisher Scientific	Cat# A32744
Goat anti-Rabbit IgG (H+L) highly cross-adsorbed secondary antibody, Alexa fluor plus 488	Thermo Fisher Scientific	Cat# A32731
Acetylated α-tubulin	Santa Cruz Biotechnology	Cat# sc-23950
ACE2	ProteinTech	Cat# 21115-1-AP
OCT3/4	Santa Cruz Biotechnology	Cat# sc-5279
Sec 5 (EXOC2)	Santa Cruz Biotechnology	Cat# sc-393230
SARS-CoV-2 N protein	BIO Vision	Cat# A2061-50
Bacterial and virus strains		
SARS-CoV-2 B.1.1.214 (EPI_ISL_2897162)	(Sano et al., 2022)	N/A
SARS-CoV-2 B.1.617.2 (EPI_ISL_9636792)	(Sano et al., 2022)	N/A
SARS-CoV-2 BA.1 (EPI_ISL_9638489)	This study	N/A
SARS-CoV-2 BA.2 (EPI_ISL_11900505)	This study	N/A
Biological samples		
Human iPS cells line, WTB CRISPRi gen1	(Mandegar et al., 2016)	N/A
Human airway organoids	(Sano et al., 2022)	N/A
Chemicals, Peptides, and Recombinant Proteins		
4% paraformaldehyde	FUJIFILM Wako Pure Chemical	Cat# 163-20145
ISOGEN	NIPPON GENE	Cat# 319-90211
Fetal bovine serum	Corning	Cat# 35-079-CV
TrypLE select	Thermo Fisher Scientific	Cat# 12563029
EMEM	FUJIFILM Wako Pure Chemical	Cat# 051-07615
Human airway organoids differentiation media	(Sano et al., 2022)	N/A
Stem fit AK02N	Ajinomoto	Cat# RCAK02N
Y-27632	FUJIFILM Wako Pure Chemical	Cat# 034-24024
iMatrix-511	Nippi	Cat# 892021
Puromycin	InvivoGen	Cat# 14861-71
Hygromycin B	Nacalai tesque	Cat# 09287-84
Blasticidin S	InvivoGen	Cat# 03759-71
Lipofectamine RNAiMAX	Thermo Fisher Scientific	Cat# 13778150
Opti-MEM	Thermo Fisher Scientific	Cat# 31985070
SUPERase In RNase inhibitor	Thermo Fisher Scientific	Cat# AM2696
Cytochalasin D	Sigma-Aldrich	Cat# C8273-1MG
Latrunculin B	Sigma-Aldrich	Cat# L5288-1MG
IFN-β	PeproTech	Cat# 300-02BC
IFN-ω	PeproTech	Cat# 300-02J
IFN-λ1	PeproTech	Cat# 300-02L
IFN-γ	PeproTech	Cat# 300-02

(*Continued on next page*)

Continued

REAGENT or RESOURCE	SOURCE	IDENTIFIER
Critical commercial assays		
Superscript VILO cDNA synthesis kit	Thermo Fisher Scientific	Cat# 11754250
FAST SYBR green PCR master mix	Thermo Fisher Scientific	Cat# 4385614
One Step TB green PrimeScript PLUS RT-PCR kit (Perfect Real Time)	TaKaRa Bio	Cat# RR096A
Cell counting kit-8	Dojindo	Cat# CK04-11
Experimental models: Cell lines		
African green monkey (*Chlorocebus sabaeus*): TMPRSS2/Vero cells	JCRB Cell Bank (Matsuyama et al., 2020)	Cat# JCRB1818
Experimental models: Organisms/strains		
Normal human bronchial epithelial cells (NHBE)	Lonza	Cat# CC-2540
Oligonucleotides		
Primers for quantitative PCR, see Table S2	This study	N/A
gRNA for CRISPRi experiments, see Figure 2C and Table S4	This study	N/A
Quantification of viral RNA copy number Fw (AGC CTC TTC TCG TTC CTC ATC AC	(Sano et al., 2022)	N/A
Quantification of viral RNA copy number Rv (CCG CCA TTG CCA GCC ATT C)	(Sano et al., 2022)	N/A
siGENOME non-targeting siRNA Pool	Dharmacon	Cat# D-001810-10-20
si-EXOC2 (SMARTpool)	Dharmacon	N/A
si-RAD54L2 (SMARTpool)	Dharmacon	N/A
si-ARID1A (SMARTpool)	Dharmacon	N/A
si-DRG1 (SMARTpool)	Dharmacon	N/A
Recombinant DNA		
Plasmid: pPV-EF1α-ACE2-pA	(Hashimoto et al., 2021)	N/A
Plasmid: pHL-EF1α-hcBase-A	(Ishida et al., 2018)	N/A
Plasmid: pPV-EF1α-EiP-pA	(Ishida et al., 2018)	N/A
Plasmid: pPB-TRE3G-EXOC2-V2	This study	N/A
Plasmid: PB-U6-CNKB	(Takahashi et al., 2020)	N/A
Plasmid: PB-U6-CNKH	(Takahashi et al., 2020)	N/A
Plasmid: PB-U6-CNKB encoding EXOC2	This study	N/A
Plasmid: PB-U6-CNKH encoding IFNW1	This study	N/A
Software and algorithms		
Prism 9 software v9.1.1	GraphPad Software	https://www.graphpad.com/scientific-software/prism/
Other		
QuantStudio 1 Real-Time PCR system	Thermo Fisher Scientific	N/A
StepOne Plus Real-Time PCR system	Thermo Fisher Scientific	N/A
96-well plate	Thermo Fisher Scientific	Cat# 167008
NEPA21 electroporator	Nepa Gene	N/A
Multiskan FC	Thermo Fisher Scientific	N/A
BZ-X710	KEYENCE	N/A

RESOURCE AVAILABILITY

Lead contact

Further information and requests for resources and reagents should be directed to and will be fulfilled by the Lead Contact, Kazuo Takayama (kazuo.takayama@cira.kyoto-u.ac.jp).

Materials availability

All unique reagents generated in this study are listed in the key resources table and available from the lead contact with a completed Materials Transfer Agreement.

Data and code availability

The sequence information of SARS-CoV-2 used in this study are available from the GISAID database (https://www.gisaid.org); B.1.1.214 (GISAID accession number: EPI_ISL_2897162), B.1.617.2 (EPI_ISL_9636792), BA.1 (EPI_ISL_9638489), and BA.2 (EPI_ISL_11900505). Any additional information required to re-analyze the data reported in this paper is available from the lead contact upon request.

EXPERIMENTAL MODEL AND SUBJECT DETAILS

Ethics statement

All protocols involving specimens from human subjects recruited at Kyoto University were reviewed and approved by the Institutional Review Boards of Kyoto University (approval ID: R2379-3).

Cell culture

TMPRSS2/Vero cells (Vero cells stably expressing human TMPRSS2; JCRB1818, JCRB Cell Bank) (Matsuyama et al., 2020), which were maintained with Eagle's Minimum Essential Media (EMEM, FUJIFILM Wako Pure Chemical) supplemented with 5% fetal bovine serum and 1% penicillin/streptomycin. Human iPS cells and AOs were generated according to established protocols as described below (see "human iPS cells" and "airway organoids" sections).

METHOD DETAILS

Human iPS cells

The iPS cell line WTB CRISPRi Gen1 (provided by Dr. Bruce R. Conklin, Gladstone Institutes)[9] was maintained on 0.5 μg/cm^2 recombinant human laminin 511 E8 fragments (iMatrix-511, Nippi) with StemFit AK02N medium (Ajinomoto) containing 10 μM Y-27632 (from day 0 to day 1, FUJIFILM Wako Pure Chemical). To passage the cells, iPS cell colonies were treated with TrypLE Select Enzyme (Thermo Fisher Scientific) for 8 min at 37°C. After centrifugation, the cells were seeded at an appropriate density (1.3×10^4 cells/9 cm^2) on iMatrix-511 and cultured every 6 days.

Airway organoids

Normal human bronchial epithelial cells (NHBE, #CC-2540, Lonza) were used as human bronchial basal cells in this study. AO were generated from NHBE and maintained as we previously reported.[24]

SARS-CoV-2 preparation

The severe acute respiratory syndrome coronavirus 2 (SARS-CoV-2) strains B.1.1.214 (GISAID accession number: EPI_ISL_2897162), B.1.617.2 (EPI_ISL_9636792), BA.1 (EPI_ISL_9638489), and BA.2 (EPI_ISL_11900505) were isolated from a nasopharyngeal swab sample of a coronavirus disease 2019 (COVID-19) patient. This study was approved by the research ethics committee of Kyoto University (R2379-3). All figures except Figure 3F show data for SARS-CoV-2 B.1.1.214. The virus was proliferated in TMPRSS2/Vero cells (JCRB1818, JCRB Cell Bank),[39] which were then stored at −80°C. TMPRSS2/Vero cells were cultured with Eagle's Minimum Essential Media (EMEM, FUJIFILM Wako Pure Chemical) supplemented with 5% fetal bovine serum and 1% penicillin/streptomycin. All viral infection experiments were done in a biosafety level 3 facility at Kyoto University strictly following regulations.

Viral titration of SARS-CoV-2

Viral titers were measured by a median tissue culture infectious dose (TCID50) assay. TMPRSS2/Vero cells were cultured with EMEM and seeded into 96-well cell culture plates (Thermo Fisher Scientific). The

samples were serially diluted 10-fold from 10^{-1} to 10^{-8} in the cell culture medium. Dilutions were placed onto the TMPRSS2/Vero cells in triplicate, which were then incubated at 37°C for 96 h. Cytopathic effects were evaluated under a microscope. TCID50/mL was calculated using the Reed-Muench method.

Drug or IFN treatment

AO or ACE2-expressing iPS cells cultured in a 96-well plate (2.0×10^4 cells/well) were infected with 2.0×10^3 TCID50/well of SARS-CoV-2 for 2 h and then cultured with medium containing drugs or various IFNs. Medium containing drugs or IFNs was replaced with fresh medium every day. Two days after the infection, the viral RNA copy number in the cell culture supernatant was measured by qPCR. The drugs and IFNs used in the infection experiments are summarized in Table S1.

Cell viability test

Cell viability was assessed by the Cell counting kit-8 (Dojindo). The viability of cells without DOX was taken as 100%.

Quantification of viral RNA copy number

The cell culture supernatant was mixed with an equal volume of 2×RNA lysis buffer (distilled water containing 0.4 U/μL SUPERase In™ RNase Inhibitor (Thermo Fisher Scientific), 2% Triton X-100, 50 mM KCl, 100 mM Tris-HCl (pH 7.4), and 40% glycerol) and incubated at room temperature for 10 min. The mixture was diluted 10 times with distilled water. Viral RNA was quantified using a One Step TB Green PrimeScript PLUS RT-PCR Kit (Perfect Real Time) (Takara Bio) on a StepOnePlus real-time PCR system (Thermo Fisher Scientific) or QuantStudio 1 (Thermo Fisher Scientific). The primers used in this experiment are as follows: (forward) AGCCTCTTCTCGTTCCTCATCAC and (reverse) CCGCCATTGCCAGCCATTC. Standard curves were prepared using SARS-CoV-2 RNA (10^5 copies/μL) purchased from Nihon Gene Research Laboratories.

Quantitative PCR

Total RNA was isolated from AO and human iPS cells using ISOGENE (NIPPON GENE). cDNA was synthesized using 500 ng of total RNA with a Superscript VILO cDNA Synthesis Kit (Thermo Fisher Scientific). Real-time RT-PCR was performed with SYBR Green PCR Master Mix (Thermo Fisher Scientific) using a StepOnePlus real-time PCR system or QuantStudio 1 (Thermo Fisher Scientific). The relative quantification of target mRNA levels was performed using the $2^{-\Delta\Delta CT}$ method. The values were normalized to the housekeeping gene *glyceraldehyde 3-phosphate dehydrogenase* (*GAPDH*). The PCR primer sequences are shown in Table S2.

siRNA transfection

AO were dissociated and transfected with 50 nM siRNAs (Dharmacon SMARTpool, GE Healthcare) or control siRNA (si-control; Dharmacon siGENOME Non-targeting siRNA Pool, GE Healthcare) using Lipofectamine RNAiMAX reagent.

Immunofluorescence staining

For the immunofluorescence staining of AO and human iPS cells, the cells were fixed with 4% paraformaldehyde in PBS at 4°C. After blocking the cells with PBS containing 2% BSA and 0.2% Triton X-100 at room temperature for 45 min, the cells were incubated with a primary antibody at 4°C overnight and then with a secondary antibody at room temperature for 1 h. All antibodies used in this report are described in Table S3.

ACE2-expressing iPS cells

WTB CRISPRi Gen1 were electroporated with pPV-EF1α-ACE2-A and pHL-EF1a-hcPBase-A vectors[40] using a NEPA21 electroporator (Nepa Gene), and then selected with 1 μg/mL puromycin (InvivoGen). The *piggyBac*-based ACE2-expressing plasmid, pPV-EF1α-ACE2-A, was constructed by replacing EGFP gene of pPV-EF1a-EiP-A with ACE2 gene. A *piggyBac*-based EGFP-expressing plasmid, pPV-EF1a-EiP-A, and a *piggyBac* transposase-expressing plasmid, pHL-EF1a-hcPBase-A, were kind gifts from Dr. Akitsu Hotta (Kyoto University).

Generation of EXOC2-expressing iPS cells

WTB CRISPRi Gen1 were electroporated with pPB-TRE3G-EXOC2-V2 and pHL-EF1a-hcPBase-A vectors using the NEPA21 electroporator and then selected with blasticidin S (InvivoGen). The piggyBac-based EXOC2-expressing plasmid, pPB-TRE3G-EXOC2-V2, was constructed by inserting human EXOC2 gene into multiple cloning sites of pPB-TRE3G-MCS(A)-P2A-MCS(B)V2, which was a kind gift from Dr. Takeshi Maruyama (Waseda University).

CRISPRi experiments in human iPS cells

To perform CRISPRi experiments, we used a human iPS cell line that carries a DOX-inducible KRAB-dCas9 gene expression cassette in the *AAVS1* locus (WTB CRISPRi Gen1). The sgRNA sequences were selected from a reported sgRNA sequence list.[41] A mixture of 5 sgRNAs was used to knockdown EXOC2, EXOC8, or IFNW1 expression. The sgRNA sequences used in this study are summarized in Figure 2C and Table S4. To establish sgRNA- and ACE2-expressing WTB CRISPRi Gen1 cells, the iPS cells (1×10^6 cells) were transfected with 7.5 μg PB-U6-CNKB[42] encoding EXOC2, PB-U6-CNKB encoding EXOC8, or PB-U6-CNCH[42] encoding IFNW1 sgRNA sequence and 2.5 μg pCW-hyPBase using the NEPA21 electroporator. After 10 μg/mL-blasticidin S or 10 μg/mL-Hygromysin B (Nacalai tesque) selection and single-cell cloning, mKate2-or Clover-positive WTB CRISPRi Gen1 cells were cultured with or without 1 μg/mL DOX to induce the expression of KRAB-dCas9.

QUANTIFICATION AND STATISTICAL ANALYSIS

Statistical significance was evaluated using unpaired two-tailed Student's *t*-test or one-way analysis of variance (ANOVA) followed by Tukey's post hoc tests. Statistical analyses were performed using GraphPad Prism 9. Data are representative of three independent experiments. Details are described in the figure legends.